COBEM 2025
28TH INTERNATIONAL CONGRESS OF MECHANICAL ENGINEERING
ABCM Brazilian Society of Mechanical Sciences and Engineering
28th ABCM International Congress of Mechanical Engineering
November 09-11, 2025, Curitiba-PR, Brazil

COB-2025-0018
DEVELOPMENT OF AN INFRARED SENSOR-BASED SYSTEM FOR INTERLAYER TEMPERATURE CONTROL IN CMT-BASED WIRE ARC ADDITIVE MANUFACTURING

Dainel Galeazzi
Universidade Federal de Santa Catarina – UFSC, Instituto de Soldagem e Mecatronica – LABSOLDA
daniel.galeazzi@posgrad.ufsc.br

Mateus Barancelli Schwedersky
Universidade Federal de Santa Catarina – UFSC, Instituto de Soldagem e Mecatronica – LABSOLDA
m.barancelli@ufsc.br

Regis Henrique Goncalves e Silva
Universidade Federal de Santa Catarina – UFSC, Instituto de Soldagem e Mecatronica – LABSOLDA
regis.silva@ufsc.br

Fernando Costenaro Silva
Universidade Federal de Santa Catarina – UFSC, Instituto de Soldagem e Mecatronica – LABSOLDA
fernando.costenaro@ufsc.br

Abstract. *Wire arc additive manufacturing is an emerging process that has garnered increasing attention from both industry and academia due to its capability to produce complex parts with minimal material waste and high industrial flexibility. However, to ensure that the fabricated parts are functionally applicable in industrial environments, several technological and scientific barriers must be overcome. In this context, sophisticated welding processes are commonly employed, with GMAW (Gas Metal Arc Welding), particularly its dynamic feeding variant CMT (Cold Metal Transfer), being the most utilized. Despite the sophistication of these processes, many challenges remain. One of the primary challenges in wire arc additive manufacturing is the "CAD to Part" relationship, which refers to the fidelity between the digital model (CAD) and the final produced part. Achieving this fidelity requires welding parameters to be aligned with the deposition path, thereby controlling bead geometry relative to the predetermined path. Among the parameters critical to controlling the deposition trajectory, interlayer temperature stands out due to its significant influence on both welding parameters and trajectory, as well as its impact on the mechanical and metallurgical properties of the final part. This work aims to present the development of an arc opening control system based on interpass temperature, using an infrared sensor integrated into an additive manufacturing robotic cell. To achieve this, a mapping of the GMAW-CMT welding process was initially conducted by depositing single weld beads on a plate at different temperatures to identify the threshold at which temperature significantly affects bead geometry. Subsequently, an IR sensor compatible with the function was selected, along with other necessary devices for system development (Arduino UNO R3 and Relay Module). The communication protocols required for integrating these devices with each other and with the robot controller (Yaskawa Motoman HP20D - DX100) were then identified. Finally, these devices were integrated using an algorithm developed in C#. To validate the system, a cylinder consisting of 180 layers was fabricated using the WAAM process. The system aimed to maintain consistent layer height by controlling the interpass temperature, varying the idle time. The results demonstrated that the interpass temperature has a significant influence on the weld bead geometry, the developed system provides accurate interpass temperature measurement and effective control of layer height through interpass temperature monitoring, thus achieving improved accuracy in the CAD to Part relationship.*

Keywords: *WAAM-CMT; Robotics; Automation; Welding; Industry 4.0.*

1. INTRODUCTION

Wire arc additive manufacturing (WAAM) is an emerging manufacturing process that has gained significant attention due to its ability to produce complex, customized parts with intricate geometries by combining different materials and mechanical properties. Additionally, WAAM stands out for its higher productivity and lower equipment costs compared to laser-based additive manufacturing processes.

This process focuses on fabricating components through the controlled deposition of material along a predefined path, where fusion is achieved by means of an electric arc.

In this context, welding processes with advanced embedded technology are extensively used in additive manufacturing due to their high level of control over metal transfer and welding variables. One standout method is the CMT (Cold Metal Transfer) variant of the GMAW (Gas Metal Arc Welding) process, which features dynamic wire

feeding. As highlighted in the literature, the CMT system offers geometric control of the weld bead, high arc stability, and enables high deposition rates — all desirable characteristics for part fabrication via additive manufacturing (Ali et al., 2019; Furukawa, 2006; Mvola, Kah e Layus, 2018; Posch, Chladil e Chladil, 2017; Yang et al., 2019). However, even with reliable equipment and processes, additive manufacturing operations require more than just welding parameter control — they demand comprehensive control of heat input, interlayer temperature, trajectory planning, and other variables. Neglecting these aspects can compromise the success of additive manufacturing operations (Bai et al., 2018; Ding et al., 2014, 2015a; b; c; Mehnen et al., 2011).

One of the main challenges in additive manufacturing is the CAD-to-part relationship — that is, the integration between computer-aided design (CAD) and the physical fabrication of the part. This relationship involves several critical stages, including process planning and parameterization — i.e., the welding parameters and operational guidelines that must be programmed into the toolpath to ensure the final part meets dimensional and mechanical requirements (Ding et al., 2015a, 2016; Wang et al., 2021).

Given this scenario, it is essential to map and understand the physical phenomena associated with the metal transfer process and its impact on the weld bead profile. This knowledge allows the implementation of control strategies to minimize process variation. Process monitoring and control can be achieved using a variety of sensors.

The present study focuses on temperature sensors, specifically on controlling the interlayer temperature, which must be kept consistent to maintain the bead geometry and metallurgical characteristics throughout the entire deposition process, in addition to preventing welding defects such as porosity and cracking. For example, Scotti, (2019) employed a temperature sensor (pyrometer) to monitor and control the interlayer temperature during the fabrication of thin aluminum walls. This control enabled consistent bead geometry throughout the deposition, regardless of temperature variation.

Similarly, Xia et al., (2020) reviewed WAAM monitoring and control methods, highlighting the use of thermal sensors to improve part quality. Infrared thermography sensors and pyrometers are used to capture the thermal profile of the melt pool, assisting in temperature control and defect detection such as porosity and cracks. The study points out that thermal variation influences microstructures and mechanical properties, making thermal monitoring essential to ensure process stability and material integrity.

Likewise, Chabot, Rauch e Hascoët, (2021), presented a thermal monitoring system for direct energy deposition (DED) processes, including LMD (Laser Metal Deposition) and WAAM. Using an infrared camera, the system monitors the part's temperature distribution to assess heat accumulation and predict microstructural changes. The study defines a High-Temperature Zone (HTZ) as an indicator of overheating, allowing real-time adjustments such as interlayer waiting times to reduce residual stresses and thermal distortion, ultimately improving part quality.

Considering the importance of interlayer temperature monitoring and control, this work aims to present the development of an arc-opening control system based on interlayer temperature monitoring using an infrared sensor integrated into a robotic additive manufacturing cell.

2. MATERIALS AND METHODS

To achieve the main objective of this study, a feasibility analysis was initially carried out. This involved investigating the communication method required with the robot controller and identifying the necessary electronic components. Additionally, the communication protocols needed for integration—both between the devices themselves and between the devices and the robot controller—were evaluated. The electronic components used in this phase included: an OMEGA infrared temperature sensor, model OS-MINUSB-SN201; an Arduino UNO R3 microcontroller board; and a relay module. These components were integrated using an algorithm developed in C# on Microsoft's Visual Studio 2022 platform. The technical specifications of the equipment used are presented in Table 1. Furthermore, a support bracket was designed to mount the sensor onto the robotic arm. This bracket was modeled using CAD software and manufactured through 3D printing with polymer materials.

Table 1. Technical specifications of the equipment used in the prototype.

Item	Device	Description
a)		**OMEGA Temperature Sensor, OS-MINUSB-SN201** • Sensor type: Photonic; • Acquisition rate: 8 Hz; • Field of view: 20:1; • Spot diameter: 36 mm at 500 mm from the part; • Temperature range: -20 to 1000 °C; • Dimensions: ø18 mm x 45 mm; • Power supply: 5 VDC (via USB); • Communication: Modbus over serial line.

b)	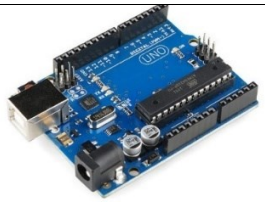	**Arduino UNO R3 Module** • Microcontroller: ATmega328; • Clock speed: 16 MHz; • Digital I/O pins: 20 (6 usable as PWM); • Analog ports: 6; • Operating voltage: 5 V; • Dimensions: 53.4 x 86.6 mm.
c)	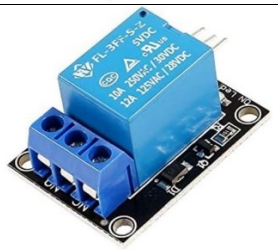	**Relay Module, model FL-3FF-S-Z** • Operating voltage: 5 VDC; • Controls loads up to 220V AC; • Nominal current: 71.4 mA; • Pin configuration: Normally Open, Normally Closed, Common; • Output voltage: 28 VDC at 10A / 250VAC at 10A / 125VAC at 15A; • Response time: 5–10 ms; • Dimensions: 26 mm x 33 mm x 18 mm

Before the validation experiments, the sensor emissivity was calibrated over a temperature range of 50 to 400 °C. A contact thermocouple and a flat steel plate manufactured by WAAM were used for calibration. The plate was heated to different temperatures and monitored by a mobile thermocouple device. The IR sensor was positioned at the same location as the thermocouple, and the emissivity was adjusted until the temperature measured by the IR sensor matched that of the thermocouple. This procedure was repeated for each reference temperature (50, 100, 200, 300, and 400 °C). Although slight variations in emissivity were observed across the range, an average value of 0.78 was adopted for all measurements.

The system was validated by printing a cylindrical part with an average diameter of 60 mm, using 180 layers. This setup required 45 pauses per quadrant. After the deposition of each layer, when the robot stopped at the endpoint, the sensor was activated to monitor the workpiece temperature. Simultaneously, a mobile contact thermocouple was placed near the sensor ROI, and the temperature values were recorded. This procedure aimed to verify the accuracy of the sensor calibration, which represents the main objective of this study.

The layer increment was 2.3 mm, and the interlayer temperature was programmed to 150 °C. The chosen path divided the base circle into four quadrants, offset by 90°. Each layer started and ended at the same point, ensuring continuity. Additionally, a 180° offset was programmed between the end of one layer and the start of the next, alternating the welding direction between clockwise and counterclockwise. This strategy allowed for a uniform and symmetrical distribution of layers around the cylinder. Figure 1 schematically illustrates the experiment.

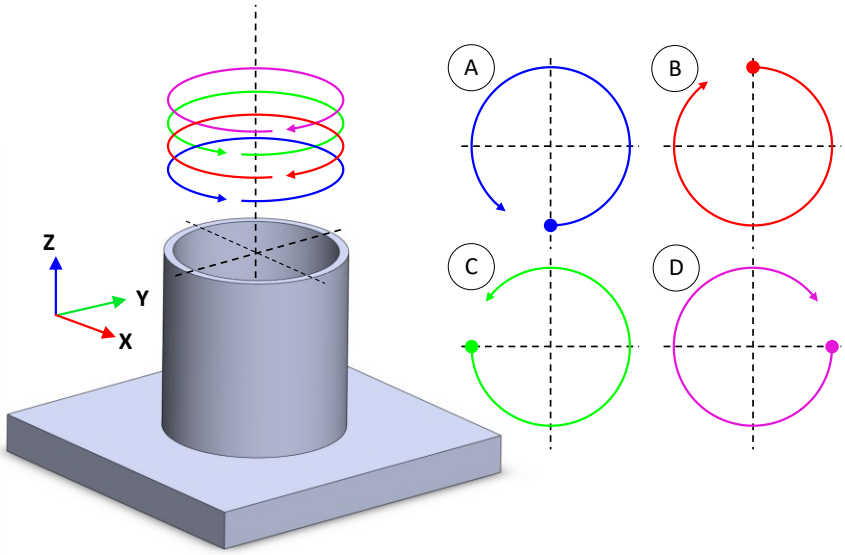

Figure 1. Schematic representation of the experiment for validating the temperature control system.

The experiment evaluated the sensor's performance under different operating conditions. At the end of each layer, temperature readings were taken in the following scenarios: (1) front-facing readings with the sensor directly in front of the part, (2) lateral readings capturing half of a section, and (3) obstructed readings with a nearby object partially in the field of view. During the experiment, the welding torch remained perpendicular to the substrate, while the sensor's field of view stayed parallel to the Y-axis displacement, ensuring a measurement plane that was parallel to the sensor's field

of view but inclined at 37°. This configuration minimized interference from obstacles and enabled measurements on multi-faceted parts. Figure 2 illustrates the measurement scenarios.

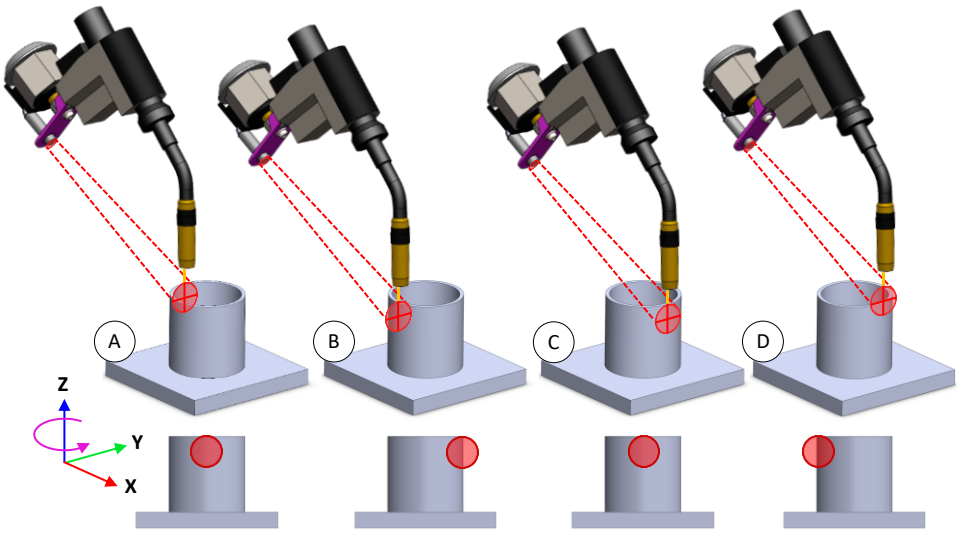

Figure 2. Schematic representation of the measurement scenarios adopted in the experiment for validating the temperature control system.

Temperature monitoring during the experiment was conducted using the infrared sensor in conjunction with a type K contact thermocouple. The recorded temperature value was the first measurement below the defined reference temperature. The sensor was configured to read the maximum temperature reached within a one-second sampling period.

In addition to temperature monitoring, the average height of each deposited layer was also evaluated. For this, four measurements were taken per layer—one in each quadrant—using a Mitutoyo digital caliper with a resolution of 0.01 mm. The adopted method consisted of measuring the total height of the cylinder and subtracting the height of the previous layer, as defined by Equation (1).

$$\overline{A_c} = \bar{A}_i - \bar{A}_{i-1}, \tag{1}$$

Where A_c is the average height of the current layer (mm), A_i is the average current height of the cylinder (mm), and A_{i-1} is the average height of the previous layer (mm).

Based on the results, a detailed analysis of the temperature control system's performance and its influence on weld bead geometry was carried out.

3. RESULTS AND DISCUSSION

To maximize the performance of the system and avoid unnecessary interruptions during the deposition process, an automated operation control system based on the part's temperature was implemented. For this purpose, a temperature sensor was integrated into the welding cell, as described in the methodology.

First, the sensor manufacturer's manual was consulted to identify its main features. It was found that the sensor operates in a time-based mode, meaning that the reported temperature values result from a predefined sampling period. The minimum and maximum temperature features correspond to the lowest and highest readings during the sampling time, respectively, while the average temperature is calculated as the mean of all values recorded during that period.

Next, the sensor's communication protocol was mapped and identified as MODBUS over USB. Based on this, the required addresses for algorithm development were defined, including the read/write register, emissivity, minimum temperature, average temperature, maximum temperature, and sampling time.

Upon analyzing the DX100 controller integrated with the Motoman HP20D robotic cell, it was verified that the controller has a comprehensive set of digital input/output (I/O) ports. However, it was also observed that the controller cannot receive analog signals (e.g., a temperature signal from the IR sensor) to perform specific conditional operations. To overcome this limitation, an algorithm was developed to integrate the temperature sensor with the controller. The temperature readings were processed and converted into digital signals based on defined conditions.

To send a signal to the controller and activate a digital input, a 24 V signal must be applied to the desired port, as this voltage is already available on at least four I/O unit ports. When creating a digital input signal, a port is enabled through the Universal INPUT function in the robot's IN/OUT control module. For instance, A1 and B7 represent the User Input

IN10 port, with A1 corresponding to the IN10 port and B7 to the 24 V signal. Figure 3 shows the appearance of the IN10 port when activated.

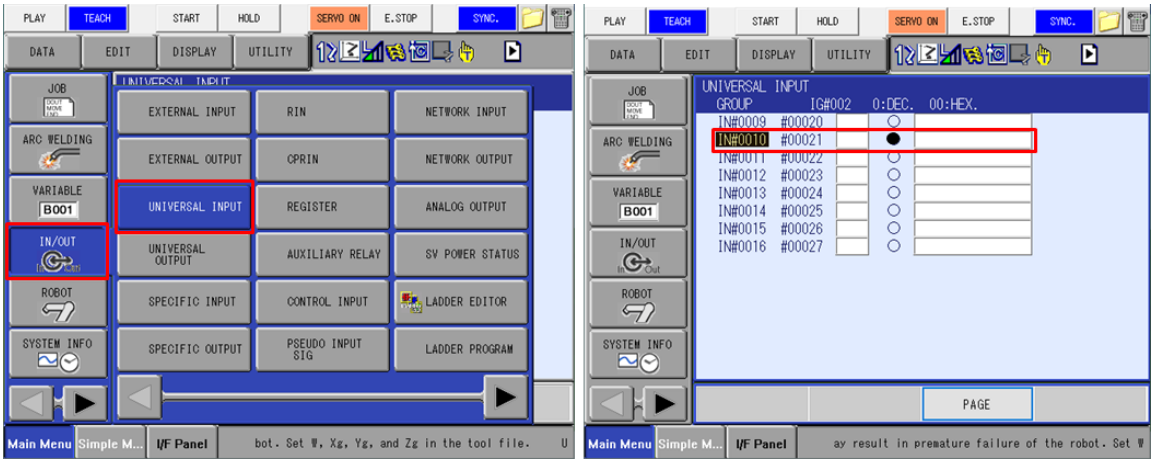

Figure 3. Path to locate the digital input.

To send the signal generated by the algorithm and activate the digital input, an integrated circuit (IC) must receive the signal via serial connection and transmit it to the controller. However, in this case, it is essential to electrically isolate the IC from the controller to prevent voltage interference. To meet these requirements, an Arduino UNO was used as the IC and a relay module as the isolation component. The Arduino receives the serial signal and activates the relay module, which electrically isolates the controller's circuit, ensuring proper operation.

Before reading and acting on the temperature signal, the algorithm performs a pre-configuration step to set the emissivity and sampling time. For the temperature range between 50 °C and 400 °C, and considering the type of surface, an emissivity value of 0.78 was established based on comparative readings between the sensor and a type K thermocouple. A sampling time of one second was defined, allowing for five measurements considering the sensor's maximum acquisition rate of 5 Hz. These parameters were chosen to ensure precise and reliable operation within the desired temperature range.

The algorithm is based on comparing the measured temperature with a reference value. It checks whether the temperature is above or below the threshold and plans accordingly. This decision is communicated to the Arduino via serial connection by sending a "1" or "0" signal. A value of "1" indicates that the relay module connected to the input port should be activated, powering the respective input on the controller. Conversely, a "0" keeps the relay off or deactivates it, thereby turning off the corresponding controller input. A flowchart of the algorithm is shown in Figure 4.

This digital signal generated within the controller can be used in the programming environment, which uses the native Inform III language, to control the execution of the operation through specific commands such as WAIT or UNTIL. In this study, the WAIT command was used, which instructs the robot to wait until the controller input is activated, i.e., until the part's temperature is below the defined reference. Temperature monitoring plays a crucial role here, enabling accurate interlayer temperature control during the additive manufacturing process, thereby mitigating geometric variations caused by overheating.

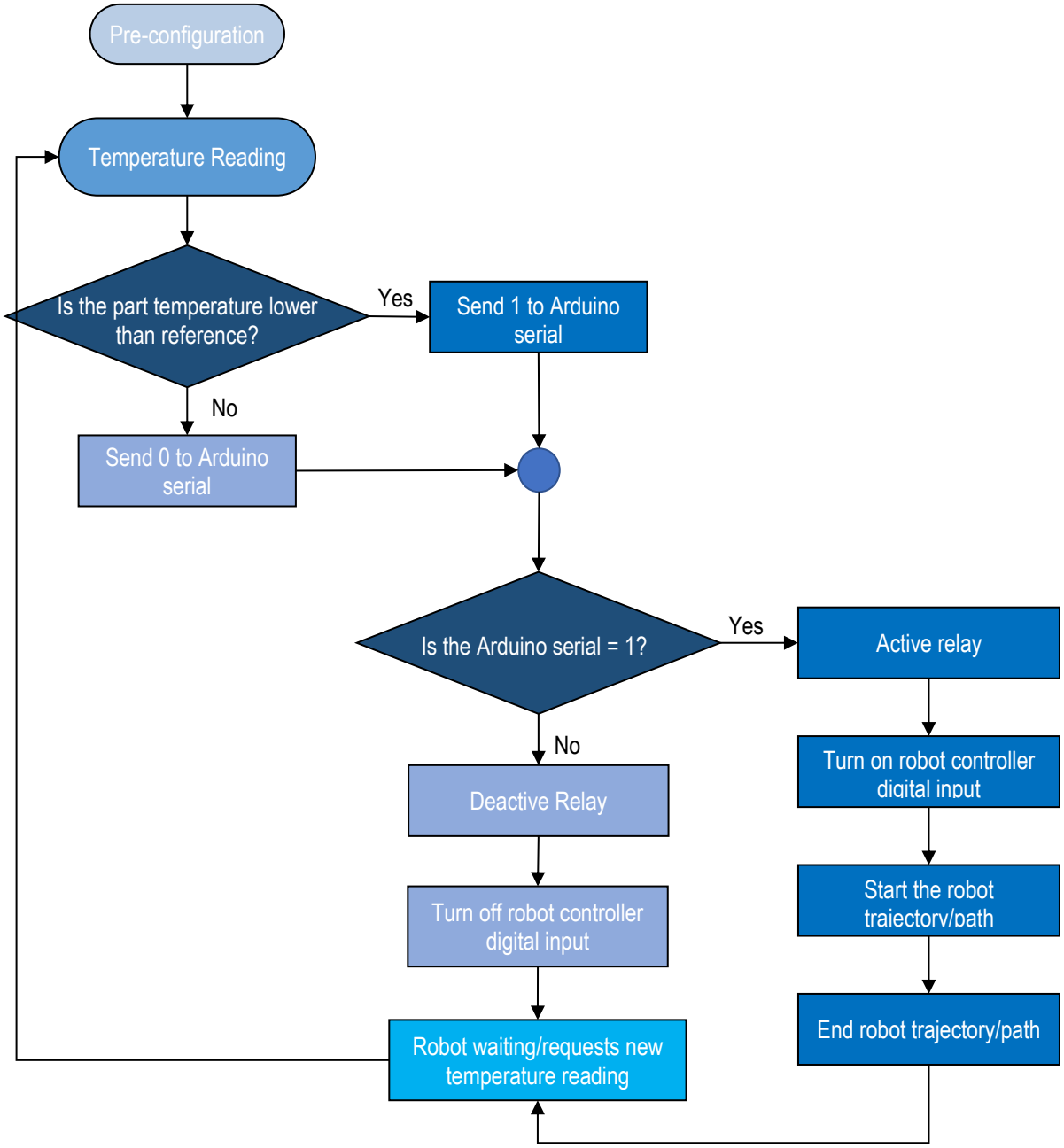

Figure 4. Flowchart of the interlayer temperature control algorithm operation.

The sensor's position relative to the part was a key consideration in this study. The most suitable location, ensuring both sensor safety and reliable readings regardless of robot orientation, was identified as the sixth axis of the robot. This placement allows the sensor to read the region of interest (ROI) from any position without exposing it to excessive heat, weld spatter, or potential oxide particles from the part. This ensures the sensor's integrity and contributes to reliable temperature measurements throughout the process.

The adopted infrared sensor has a distance-to-spot-size ratio of 20:1, meaning the spot diameter is 20 times smaller than the measurement distance. Based on this ratio and the chosen position, a specific bracket was designed to ensure temperature acquisition below the maximum CTWD (Contact tip workpiece distance) limit of 20 mm. A distance of 305 mm was defined, resulting in an approximate spot size of 27 mm. CAD views of this configuration are shown in Figure 5.

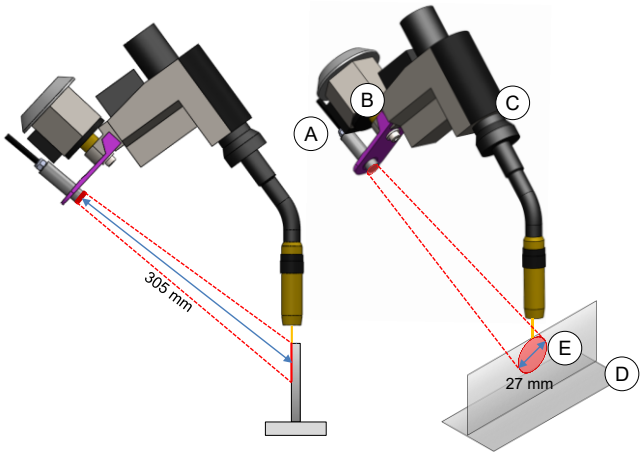

Figure 5. 3D design scheme of the infrared temperature sensor mount, where: A) OMEGA OS-MINIUSB temperature sensor, B) Temperature sensor bracket, C) Fronius Robact torch, D) Workpiece, and E) Spot size.

The holder was manufactured using 3D printing with PLA as the base material. PLA was selected for its mechanical and thermal properties, which are suitable for this application. Figure 6 shows the final bracket installation and the successful integration of the sensor into the robot structure.

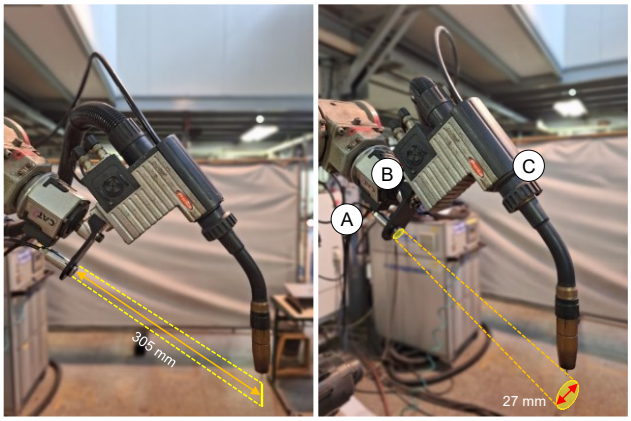

Figure 6. Result of the holder fabrication and temperature sensor assembly.

The temperature control system was validated by printing a cylindrical part 60 mm in diameter and 180 layers in height, as described in the methodology. A photo of the final printed part is shown in Figure 7.

Figure 7. Surface appearance of the printed cylinder using the temperature control system.

The goal of this experiment was to control the geometric variation of the layers by maintaining a constant interlayer temperature. Additionally, the study aimed to determine whether the temperature reading was influenced by the quadrant used for measurement at the end of each layer.

The results showed no significant difference ($p > 0.05$) between the temperature readings obtained from the IR sensor and the thermocouple, regardless of the quadrant. This can be seen in the graphs in Figure 8, which show the temperature readings for each quadrant.

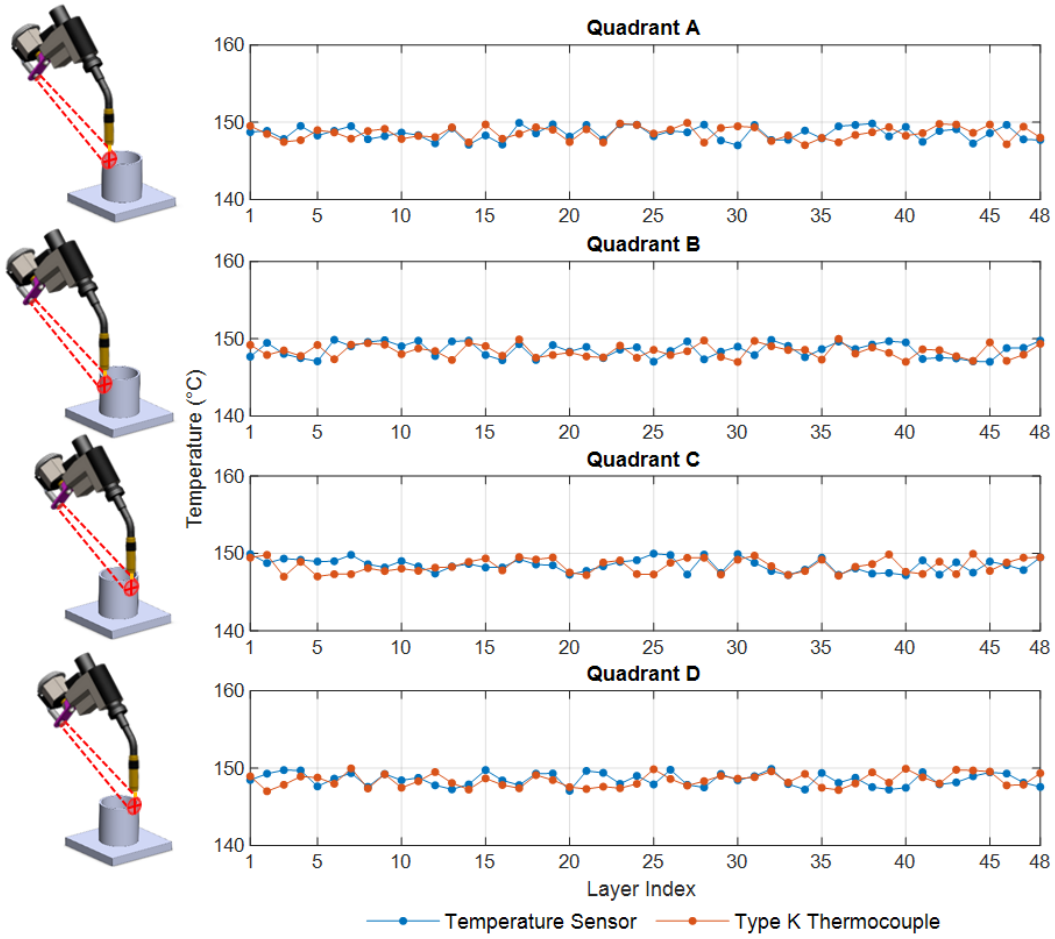

Figure 8. Temperature values for each quadrant of the deposited part.

Besides, the variation in layer height, considering the sample set, was not statistically significant ($p > 0.05$). The average layer height was 2.31 mm with a standard deviation of 0.03 mm. This result aligns with expectations, as the interlayer temperature and related parameters were kept constant. Figure 9 presents the graph of the average height measurements per layer.

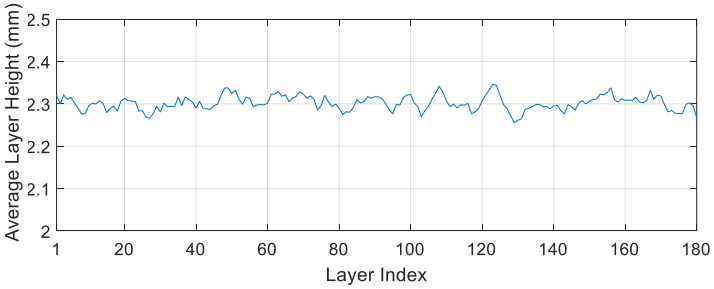

Figure 9. Average layer height measurements for the printed cylinder.

In summary, the interlayer temperature control system demonstrated robustness in temperature measurement accuracy. Furthermore, the combined effect of temperature control and the cooled base enabled the fabrication of a part approximately 415 mm of height, with low standard deviation between layers. Therefore, the system composed of a cooled base and interlayer temperature control algorithms proved effective for automating the WAAM process, contributing to process efficiency and accuracy. These results are consistent with findings by Huang, et al. (2022), Ermakova, et al. (2020), Silvestru, et al. (2021) e Silva, et al. (2019), who reported similar improvements in bead geometry control using comparable methods.

4. CONCLUSION

- A control system for interlayer temperature in wire arc additive manufacturing processes was developed and validated, based on the integration of an infrared sensor into a robotic cell using the GMAW-CMT process.
- The algorithm developed in C# enabled continuous temperature reading, comparison with a reference value, and the transmission of digital signals to the robot controller for automatic arc activation management.
- The strategic positioning of the sensor, combined with a 3D-printed mounting bracket, ensured stable and safe measurements even in environments with spatter and excessive heat.
- Tests performed during the printing of a 180-layer cylindrical part demonstrated that the system was able to maintain the interlayer temperature within the specified range (150 °C), resulting in layers with consistent average height and low standard deviation (2.31 ± 0.03 mm).
- Temperature readings from the infrared sensor were statistically equivalent to those obtained using a thermocouple, confirming the system's measurement accuracy.
- The proposed system proved to be robust and suitable for automating WAAM processes, contributing to greater geometric repeatability between layers and improved CAD-to-part fidelity.
- The implementation of this type of control reinforces the alignment of additive manufacturing with Industry 4.0 principles, promoting smarter and more reliable production systems.

5. ACKNOWLEDGEMENTS

The authors would like to thank the Welding and Mechatronics Laboratory – LABSOLDA at the Federal University of Santa Catarina (UFSC) for the technical support and infrastructure provided during the development of this work. They also extend their gratitude to Petrobras and Shell for the financial support and encouragement of applied research in welding and additive manufacturing processes. This study was partially funded by the Brazilian Federal Agency for Support and Evaluation of Graduate Education (CAPES).

6. REFERENCES

Ali, Y., Qureshi, A.J., Hassanin, H., Essa, K., Arif, M. and Al-Ahmari, A.M., 2019. "*Wire arc additive manufacturing of hot work tool steel with CMT process*". Journal of Materials Processing Technology, Vol. 269, pp. 109–116.

Arduino, n.d. Arduino UNO R3 - Product Reference Manual. [no place]: [no publisher].

Bai, X., Cong, B., Ding, D., Han, J., Zhang, H. and Zhao, Z., 2018. "*Numerical analysis of heat transfer and fluid flow in multilayer deposition of PAW-based wire and arc additive manufacturing*". International Journal of Heat and Mass Transfer, Vol. 124, pp. 504–516.

Chabot, A., Rauch, M. and Hascoët, J.-Y., 2021. "*Novel control model of Contact-Tip-to-Work Distance (CTWD) for sound monitoring of arc-based DED processes based on spectral analysis*". The International Journal of Advanced Manufacturing Technology, Vol. 116, No. 11–12, pp. 3463–3472.

Ding, D., Pan, Z., Cuiuri, D. and Li, H., 2014. "*A tool-path generation strategy for wire and arc additive manufacturing*". International Journal of Advanced Manufacturing Technology, Vol. 73, No. 1–4, pp. 173–183.

Ding, D., Pan, Z., Cuiuri, D. and Li, H., 2015a. "*A practical path planning methodology for wire and arc additive manufacturing of thin-walled structures*". Robotics and Computer-Integrated Manufacturing, Vol. 34, pp. 8–19.

Ding, D., Pan, Z., Cuiuri, D. and Li, H., 2015b. "*A multi-bead overlapping model for robotic wire and arc additive manufacturing (WAAM)*". Robotics and Computer-Integrated Manufacturing, Vol. 31, pp. 101–110.

Ding, D., Pan, Z., Cuiuri, D. and Li, H., 2015c. "*Wire-feed additive manufacturing of metal components: technologies, developments and future interests*". International Journal of Advanced Manufacturing Technology, Springer London.

Ding, D., Pan, Z., Cuiuri, D. and Li, H., 2016. "*Bead modelling and implementation of adaptive MAT path in wire and arc additive manufacturing*". Robotics and Computer-Integrated Manufacturing, Vol. 39, pp. 32–42.

Ermakova, A., Mehmanparast, A., Ganguly, S., Razavi, N. and Berto, F., 2020. "*Investigation of mechanical and fracture properties of wire and arc additively manufactured low carbon steel components*". Theoretical and Applied Fracture Mechanics, Vol. 109, 102685.

Furukawa, K., 2006. "*New CMT arc welding process – welding of steel to aluminium dissimilar metals and welding of super-thin aluminium sheets*". Welding International, Vol. 20, No. 6, pp. 440–445.

Huang, C., Kyvelou, P., Zhang, R., Ben Britton, T. and Gardner, L., 2022. "*Mechanical testing and microstructural analysis of wire arc additively manufactured steels*". Materials & Design, Vol. 216, 110544.

Mehnen, J., Ding, J., Lockett, H. and Kazanas, P., 2011. "*Design for Wire and Arc Additive Layer Manufacture*". In: Global Product Development. Springer Berlin Heidelberg, pp. 721–727.

Mvola, B., Kah, P. and Layus, P., 2018. "*Review of current waveform control effects on weld geometry in gas metal arc welding process*". The International Journal of Advanced Manufacturing Technology, Vol. 96, No. 9–12, pp. 4243–4265.

Ningbo Floiroshing Precision Electron, n.d. FL-3FF PC Board Relay. [no place]: [no publisher].

Omega, n.d. USB Infrared Temperature Sensor for Benchtop, Laboratory and Education. [no place]: [no publisher].

Posch, G., Chladil, K. and Chladil, H., 2017. "*Material properties of CMT—metal additive manufactured duplex stainless steel blade-like geometries*". Welding in the World, Vol. 61, No. 5, pp. 873–882.

Scotti, A., 2019. "*The Potential of IR Pyrometry for Monitoring Interpass Temperature in Wire + Arc Additive Manufacturing*". Evolutions in Mechanical Engineering, Vol. 3, No. 1, pp. 1–5.

Silva, L.J., Reis, R.P. and Scotti, A., 2019. "*The Potential of IR Pyrometry for Monitoring Interpass Temperature in Wire + Arc Additive Manufacturing*". Evolutions in Mechanical Engineering, Vol. 3, pp. 1–5.

Silvestru, V.-A., Ariza, I., Vienne, J., Michel, L., Aguilar Sanchez, A.M., Angst, U., Rust, R., Gramazio, F., Kohler, M. and Taras, A., 2021. "*Performance under tensile loading of point-by-point wire and arc additively manufactured steel bars for structural components*". Materials & Design, Vol. 205, 109740.

Wang, Z., Cong, B., Zhang, H., Bai, X., Song, K., Ding, D. and Zhao, Z., 2021. "*Prediction of bead geometry with consideration of interlayer temperature effect for CMT-based wire-arc additive manufacturing*". Welding in the World, Vol. 65, No. 12, pp. 2255–2266.

Xia, C., Pan, Z., Polden, J. and Li, H., 2020. "*A review on wire arc additive manufacturing: Monitoring, control and a framework of automated system*". Journal of Manufacturing Systems, Vol. 57, pp. 31–45.

Yang, Q., Fan, C., Huang, X., Zhang, Y., Wu, B., Lin, S. and Zhang, X., 2019. "*Microstructure and mechanical properties of AlSi7Mg0.6 aluminum alloy fabricated by wire and arc additive manufacturing based on cold metal transfer (WAAM-CMT)*". Materials, Vol. 12, No. 16.

7. RESPONSIBILITY NOTICE

The authors are the only responsible for the printed material included in this paper.